On First-Order Markov Modeling for the Rayleigh Fading Channel

Christopher C. Tan, *Member, IEEE*, and Norman C. Beaulieu, *Fellow, IEEE*

***Abstract*—Recent models for the received signal amplitude of the flat-fading channel that use first-order finite-state Markov chains are examined. The stochastic properties of a proposed first-order model based on these recent models are examined. The limitations of using an information theoretic metric, which is sometimes used to justify a first-order Markov chain as a sufficient model for very slowly fading channels, are discussed. A simple method of qualitatively comparing autocorrelation functions is instead proposed.**

The usefulness of the first-order Markov chain in representing the flat-fading channel is examined by looking at two specific problems in wireless system applications that represent two disparate cases. The first case involves analysis over a short duration of time, relative to the inverse of the normalized Doppler frequency, while the second involves analysis over a long duration of time. Contrary to recent reports, the results indicate that first-order Markov chains are not generally suitable for very slowly fading channels. Rather, first-order Markov chains can be suitable for very slowly fading applications, which require analysis over only a short duration of time.

***Index Terms*—Fading channels, Markov processes, modeling, Rayleigh channels.**

I. INTRODUCTION

CLARKE [1] has proposed a statistical model for the received signal amplitude of the flat-fading channel based on scattering propagation. Gans [2] has further shown that in the case of isotropic, two-dimensional scattering with an omnidirectional receiving antenna, the quadrature Gaussian processes representing the fading have autocorrelation function (ACF) given by

$$R_X(\tau) = b_0 J_0(2\pi f_D \tau)$$

where b_0 is the variance of the underlying Gaussian process, f_D is the maximum Doppler frequency, and $J_0(\cdot)$ is the Bessel function of the first kind of order zero [3, eq. (9.1.12)]. Let a complex, stationary, Gaussian process have quadrature components that are mutually independent, zero mean, with identical ACF, $R_X(\tau)$. The envelope of this complex Gaussian process is a stationary process whose first-order distribution is Rayleigh, with ACF [4, p. 170]

$$R_R(\tau) = \frac{\pi b_0}{2}\, {}_2F_1\left(-\frac{1}{2}, -\frac{1}{2}; 1; R_X(\tau)^2\right) \qquad (1)$$

where ${}_2F_1(\cdot, \cdot; \cdot; \cdot)$ is the hypergeometric function [3, ch. 15]. Such processes are called Rayleigh processes. We will call this fading model the isotropic scattering, omnidirectional receiving antenna (ISORA) model and denote it by random process $R(t)$.

Other models with Ricean or Nakagami-m first-order densities [5], or different ACFs [6], [7], have been used for the flat-fading channel. We use the ISORA model throughout this paper because of its widespread applicability and acceptance [8], but our analysis remains general enough in principle to be used for these other models as well.

Recently, finite-state Markov chains have been proposed to model the flat-fading channel, with states representing discrete, nonoverlapping intervals of the received signal envelope's amplitude. We call these models amplitude-based finite-state Markov chains (AFSMCs).

Swarts and Ferreira [9] use a first-order AFSMC based on simulation statistics to determine soft-decision statistical distributions for slowly fading channels. They compare distributions for a first-order AFSMC with a software simulator to show the general usefulness of AFSMCs in modeling the fading channel. However, Swarts and Ferreira's software simulator is already known to be a Markov process [10], [11] and is different from the ISORA model.

Wang and Moayeri [12], [13] further the model in [9] by using analytical first-order statistics to calculate model parameters. Wang and Chang [14] propose a mutual information metric to mathematically demonstrate that a first-order AFSMC is sufficient to model very slowly fading channels for any application, and that the improvements of a second- or higher-order AFSMC are negligible. Zorzi *et al.* [15] derive the data-link performance of ARQ protocols as an application of this binary Markov model, and use this mutual information metric to show that a first-order binary Markov chain that models the received signal amplitude is of sufficient order. Two other papers employ AFSMC structures, presumably independently of the above four papers. Steffan [16] uses an AFSMC to analytically determine the mean inter-error time and the mean number of errors in a time interval. Bischl and Lutz [17] use a first-order AFSMC to determine block-error rates.

The AFSMC has thus gained some acceptance and seems to be finding a growing number of applications. Goldsmith and Varaiya give the correlated Rayleigh channel as an example of a

Paper approved by Z. Kostic, the Editor for Wireless Communication Theory of the IEEE Communications Society. Manuscript received July 12, 1998; revised January 15, 2000.

C. C. Tan was with the Department of Electrical and Computer Engineering, Queen's University, Kingston, ON K7L 3N6, Canada. He is now with Calimetrics, Inc., Alameda, CA 94501–2274 USA (e-mail: c.tan@ieee.org).

N. C. Beaulieu was with the Department of Electrical and Computer Engineering, Queen's University, Kingston, ON K7L 3N6, Canada. He is now with the Department of Electrical and Computer Engineering, University of Alberta, Edmonton, AB T6G 2G7, Canada (e-mail: beaulieu@ee.ualberta.ca).

Publisher Item Identifier S 0090-6778(00)10895-5.

valid finite-state Markov chain [18]. Babich and Lombardi develop Markov models for the indoor propagation channel based in part on Wang and Chang's information theoretic metric [19]. They also verify a multi-threshold success/failure process for the Rayleigh channel based in part on the same metric [20]. The binary Markov model introduced by Zorzi *et al.* is used for error modeling of the Network File System (NFS) protocol over wireless links by Dube *et al.* [21] and in error control and energy consumption analyses in nomadic computing systems by Zorzi and Rao [22]. Li and Goldsmith use the first-order AFSMC to help design a decision-feedback maximum-likelihood decoder [23].

A first-order AFSMC is analytically tractable, and may generate closed-form results easily. Work has been done to examine higher-order AFSMCs as well. Babich *et al.* look at variable-order models for the fading channel for slowly to medium fading channels [24]. Turin has similarly used hidden Markov models of greater order to model the fading channel [25]. As the order of the model increases, so does the complexity and intractability of the model. As an example, for a first-order AFSMC all model parameters can be analytically determined easily, which is not the case for a second-order AFSMC [26]. As indicated above, a majority of the literature focuses only on first-order AFSMCs presumably because of their simplicity. This paper addresses the issue of the limitations of a first-order AFSMC fading model, when used for bit-level models.[1]

This paper has the following organization. We propose a first-order AFSMC in Section II, based on some of the best aspects of the models presented in [9]–[15]. In Section III, we determine some limitations of using this first-order AFSMC to model the ISORA fading channel. We first examine the information theoretic metric of [14]. We then propose an alternate method of determining when the AFSMC models the ISORA channel accurately. We test that our first-order AFSMC is stationary, then determine the ACF of the underlying Gaussian process. We show the ACF of the first-order AFSMC is markedly different from the ACF of the ISORA fading model. Section IV examines how useful this model is in representing the ISORA fading channel. We look at two specific problems in wireless system applications and compare results obtained using the AFSMC model with results obtained using the ISORA fading channel. Our conclusions are given in Section V.

II. A First-Order Markov Model

A first-order Markov chain is defined by its initial-state occupancy probabilities and its transition probabilities [27]. We denote our discrete-time Markov chain by $\{R_n\}$ for discrete times $n = 0, 1, \ldots, \infty$. The received signal amplitude space from zero to finite maximum amplitude M is partitioned into N intervals. The thresholds of these intervals are denoted by τ_i, $i = 0, \ldots, N$, such that $\tau_0 = 0$ and $\tau_N = M$. We assign the midpoint of the interval as the representative value of each state r_k, $k = 1, \ldots, N$. Fig. 1 illustrates these definitions.

[1]As pointed out by a reviewer, the block-level Markov model can be accurate if the block length is large.

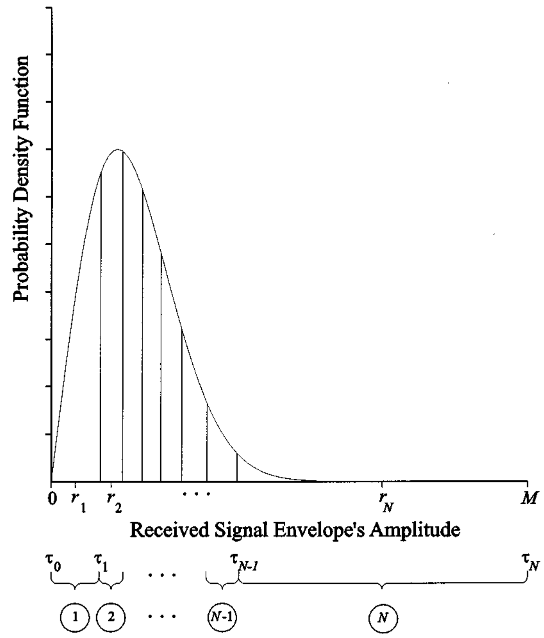

Fig. 1. Illustration of AFSMC notations and partitioning.

A. Initial-State Occupancy Probabilities

The Rayleigh probability density function (pdf) is denoted $f_R(r)$ and the Rayleigh cumulative distribution function is denoted $F_R(r)$. Without loss of generality, we assume the Rayleigh distribution has unit-variance. If our AFSMC has a standard Rayleigh first-order distribution as does the ISORA channel, we expect the initial-state occupancy probabilities π_k, $k = 1, \ldots, N$, to approach

$$\tilde{\pi}_k = \int_{\tau_{k-1}}^{\tau_k} f_R(r)\, dr$$

while satisfying

$$\sum_{k=1}^{N} \pi_k = 1. \tag{2}$$

One practical limitation of our finite-state model is that the received signal amplitude from M to infinity is not represented by a state. This introduces error in (2) if $\pi_k = \tilde{\pi}_k$, since

$$\sum_{k=1}^{N} \int_{\tau_{k-1}}^{\tau_k} f_R(r)\, dr = \int_0^M f_R(r)\, dr = F_R(M) < 1.$$

We minimize this error by setting $M = 5$ so that $F_R(M) \geq 1 - 10^{-6}$. To ensure that (2) is satisfied, we uniformly scale $\overline{\pi}$ by the sum of its elements

$$\pi_k = \frac{\tilde{\pi}_k}{\sum_{k=1}^{N} \tilde{\pi}_k}. \tag{3}$$

The states are partitioned such that the initial-state occupancy probability of all states will be the same. Thus, we solve for τ_k such that

$$\int_{\tau_{k-1}}^{\tau_k} f_R(r)\, dr = \frac{F_R(M)}{N}, \qquad i = 1, \ldots, N.$$

B. Transition Probabilities

The most direct statistics used to calculate the transition probabilities are based on the bivariate Rayleigh distribution [17], [14]. The bivariate Rayleigh distribution depends only on the correlation between adjacent samples. Define T to be the sampling period for the discrete-time fading process. In practical problems, $f_D T$ ranges from 0 to about 0.4 [26]. Two consecutive samples of the ISORA fading model's underlying Gaussian process will have correlation

$$J_1 = J_0(2\pi f_D T). \tag{4}$$

The transition probability matrix of the AFSMC, $\overline{P} = \|p_{i,j}\|_{1\le i,j\le N}$, has stationary transition probabilities (ignoring the truncation due to the finite amplitude represented by the model)

$$\tilde{p}_{i,j} = \Pr\{R_n = j | R_{n-1} = i\} \tag{5}$$

$$= \int_{\tau_{j-1}}^{\tau_j} \int_{\tau_{i-1}}^{\tau_i} f_{R_2|R_1}(r_2|r_1)\, dr_1\, dr_2$$

$$= \frac{\displaystyle\int_{\tau_{j-1}}^{\tau_j} \int_{\tau_{i-1}}^{\tau_i} f_{R_1,R_2}(r_1, r_2)\, dr_1\, dr_2}{\displaystyle\int_{\tau_{i-1}}^{\tau_i} f_R(r)\, dr} \tag{6}$$

for $1 \le i, j \le N$, where $f_{R_1,R_2}(r_1, r_2)$ is the bivariate Rayleigh joint pdf described in [4], with underlying Gaussian correlation matrix

$$\overline{M}_2 = \left\| \begin{matrix} 1 & J_1 \\ J_1 & 1 \end{matrix} \right\|.$$

The integral in (6) can be computed using the infinite series derived in [28]. We generalize the model in [9] by not restricting the number of transitions from a state.

Similar to our adjustments to the initial-state occupancy probability vector due to the finite amplitude represented by the model, we must adjust the transition probability matrix such that the rows sum to one. We uniformly scale each row by its sum

$$p_{i,j} = \frac{\tilde{p}_{i,j}}{\displaystyle\sum_{j=1}^{N} \tilde{p}_{i,j}}.$$

III. Model Assessment

In this section, we examine the information theoretic metric of [14]. We then propose an alternate method of determining the limitations of the AFSMC.

A. Information Theoretic Metric Analysis

Zorzi *et al.* [15] and Babich and Lombardi [19], [20] use an information theoretic metric developed by Wang and Chang [14] to verify that a first-order Markov chain is sufficient in representing the ISORA fading model for the applications they consider. Let R_n be the discrete-time continuous state Markov process's received amplitude at the nth time step. The first-order Markovian assumption implies that given R_{n-1}, R_n is independent of any other previous symbol R_k, $k \le n-2$.

Wang and Chang state that if the information remaining in R_n given the information corresponding to R_{n-1} is negligible, then a first-order Markov chain is a sufficient model for the channel. The authors quantify this with mutual information. They claim a first-order Markov chain is sufficient if the average conditional mutual information between R_n and R_{n-2} given R_{n-1}, $I(R_n; R_{n-2}|R_{n-1})$, is much less than the average mutual information between R_n and $\{R_{n-1}, R_{n-2}\}$, $I(R_n; R_{n-1}, R_{n-2})$. We find problems with this argument.

An important problem is that small mutual information is not a sufficient condition to indicate a process is Markov. Intuitively, one sees the ambiguity in that two samples may have little information about each other if they are either independent or highly correlated; the average conditional mutual information, $I(R_n; R_{n-2}|R_{n-1})$, approaches zero in these two distinct cases. If R_n is indeed a first-order Markov process, then the first and third samples are independent given the second sample, and $I(R_n; R_{n-2}|R_{n-1})$ is zero. However, $I(R_n; R_{n-2}|R_{n-1})$ also approaches zero if the first, second, and third samples are highly correlated. This is the case in the very slowly fading channels Wang and Chang study, where the normalized Doppler frequency is less than 0.002. Since the ISORA fading process is strictly bandlimited, we expect R_n to be very close to R_{n-1} and R_{n-2}. Note that as the three envelope samples become very close

$$\begin{aligned} &I(R_n; R_{n-2}|R_{n-1}) \\ &\quad = E\left\{\log\left(\frac{f_R(R_n, R_{n-2}|R_{n-1})}{f_R(R_n|R_{n-1}) f_R(R_{n-2}|R_{n-1})}\right)\right\} \\ &\quad \to E\left\{\log\left(\frac{\delta(R_n - R_{n-1})\,\delta(R_{n-2} - R_{n-1})}{\delta(R_n - R_{n-1})\,\delta(R_{n-2} - R_{n-1})}\right)\right\} \\ &\quad \to 0. \end{aligned}$$

Wang and Chang correctly state that the first-order Markovian assumption implies that, given the information of the state immediately preceding the current one, any other previous state should be independent of the current state. However, they then proceed to consider

$$I(R_i; R_{i-1}, R_{i-2}) = I(R_{i-1}; R_i) + I(R_{i-2}; R_i|R_{i-1}) \tag{7}$$

rather than

$$I(R_i; R_{i-1}, R_{i-2}, R_{i-3}, \ldots, R_{-\infty}). \tag{8}$$

Consideration of (7), and in particular, showing that $I(R_{i-2}; R_i|R_{i-1})$ is significantly smaller than $I(R_{i-1}; R_i)$, may have some validity in justifying whether a second-order Markov chain is marginally better than a first-order Markov chain. It cannot, however, be concluded on this basis that a higher-order Markov chain may not perform significantly better than a first-order Markov chain. Note that (8) can be written as [29, p. 22]

$$\begin{aligned} &I(R_i; R_{i-1}, R_{i-2}, R_{i-3}, \ldots, R_{-\infty}) \\ &\quad = I(R_i; R_{i-1}) \\ &\qquad + I(R_i; R_{i-2}|R_{i-1}) \\ &\qquad + I(R_i; R_{i-3}|R_{i-1}, R_{i-2}) \\ &\qquad + I(R_i; R_{i-4}|R_{i-1}, R_{i-2}, R_{i-3}) \\ &\qquad + I(R_i; R_{i-5}|R_{i-1}, R_{i-2}, R_{i-3}, R_{i-4}) + \cdots \\ &\quad = \sum_{k=1}^{\infty} I(R_i; R_{i-k}|R_{i-1}, \ldots, R_{i-k-1}). \end{aligned} \tag{9}$$

Even when $I(R_{i-2};\, R_i|R_{i-1})$ is small and the subsequent terms in (9) are monotonically decreasing, the sum of the subsequent terms can in general be significantly larger than zero, indeed even infinite. Nor is it necessarily true that the terms would be monotonically decreasing in magnitude. For example, let $f_D T = z_c/2$ where z_c is the first zero-crossing of the Bessel function $J_0(2\pi z)$. Then, the first and third samples of the underlying Gaussian processes have zero correlation and are, hence, independent. The corresponding Rayleigh samples are also independent, since they are related to the underlying Gaussian samples by a memoryless transformation. Thus, $I(R_{i-2};\, R_i|R_{i-1})$ is zero while $I(R_{i-3};\, R_i|R_{i-1},\, R_{i-2})$ is not zero (the zero-crossings of $J_0(\cdot)$ are not uniformly spaced).

B. Stochastic Analysis

We compare our first-order AFSMC to the ISORA fading model. Instead of using information theory to test our model, we look at a stochastic description of the model. Stochastic process theory gives a more complete description of the AFSMC, which allows for a clearer comparison with the ISORA fading model. We compare our AFSMC and the ISORA fading model, first by comparing first-order distributions to test whether both processes are Rayleigh distributed, then by comparing the defining parameter for each Rayleigh process, the ACF.

1) Comparison of First-Order Distributions: To calculate the first-order distribution of the first-order AFSMC, we must find the limiting probability vector. If the limiting probabilities are equal to the initial-state occupancy probabilities, then the AFSMC is stationary, and we define the first-order distribution to be the stationary distribution. Otherwise, the limiting probability vector is calculated by solving an eigenproblem of the transition probability matrix [27] using the stationary transition probabilities (6). This has been carried out numerically for a number of values of normalized Doppler frequency and Markov chain states. The initial-state probability vector agreed with the limiting probability vector for all normalized Doppler frequencies examined and for all numbers of states in the Markov chain examined. Thus, we establish confidence that the Markov chain is indeed stationary.

2) Comparison of ACFs: To calculate the ACF, we use

$$R_R[m] = \sum_{i=1}^{N}\sum_{j=1}^{N} r_i r_j \Pr\{R_m = i,\, R_0 = j\}$$
$$= \sum_{j=1}^{N} r_j \pi_j \sum_{i=1}^{N} r_i p_{i,j}^{(m)}. \tag{10}$$

As we have partitioned the states such that $\pi_j = 1/N$, the expression for the ACF can be also put into matrix form [25]

$$R_R[m] = \frac{1}{N}\,\overline{r}^\top(\overline{P}^m)^\top\overline{r} \tag{11}$$

where the state assignment vector $\overline{r}$ is defined by $\overline{r}^\top = \|r_1,\, \ldots,\, r_N\|$. Unfortunately, a general closed-form solution for the ACF in (11) seems unfeasible owing to the intractability of the Rayleigh joint pdf [26]. Therefore, we have tested the AFSMC ACF by empirically examining a number of examples.

The ISORA fading model's ACF in (1) is compared graphically with the ACF of the AFSMC computed empirically for

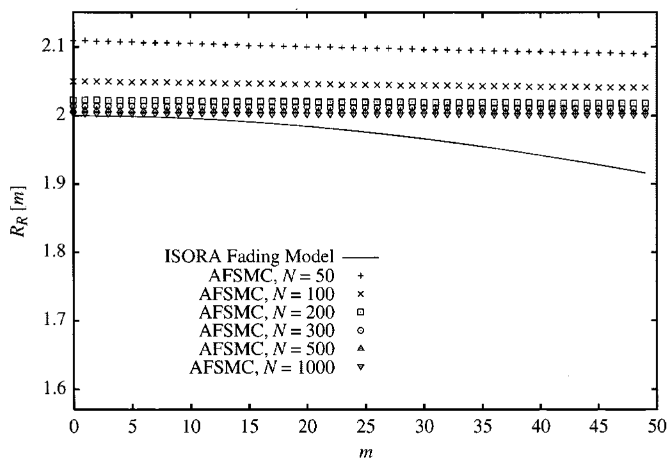

Fig. 2. Autocorrelation functions for a first-order, N-state AFSMC with $f_D T = 0.002$.

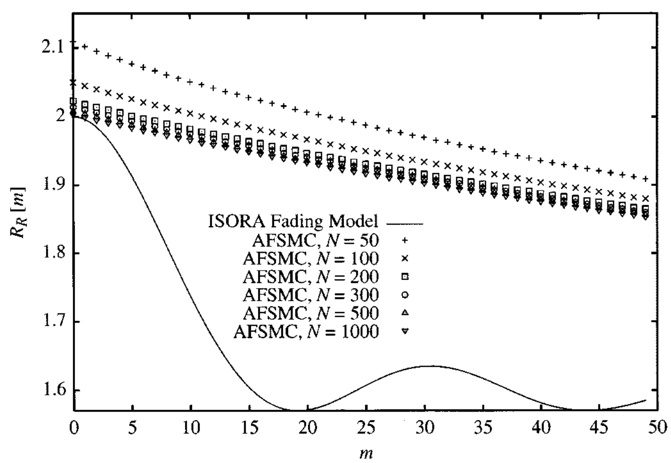

Fig. 3. ACFs for a first-order, N-state AFSMC with $f_D T = 0.02$.

$N = 50, 100, 200, 300, 500$, and 1000 states, for $f_D T = 0.002$ in Fig. 2 and $f_D T = 0.02$ in Fig. 3. In both figures, the shape of the ACF is clearly different from that of the ISORA fading model. The AFSMC ACF appears to be a monotonic decreasing exponential-like function. For large N, the only AFSMC sample points that consistently agree with the ISORA fading model's ACF are the first two sample points, $R_R[0] = {}_2F_1(-(1/2),\, -(1/2);\, 1;\, 1) = 2$ and $R_R[1] = {}_2F_1(-(1/2),\, -(1/2);\, 1;\, J_1^2)$. This is reasonable, given that the only information about the ACF input into the Markov model, through the transition probability matrix, is the value of J_1.

Several examples [26] indicate that as the number of states in the AFSMC increases, the envelope ACF converges toward

$$R_R[m] = \frac{\pi}{2}\,{}_2F_1\left(-\frac{1}{2},\, -\frac{1}{2};\, 1;\, J_1^{2m}\right) \tag{12}$$

which from (1) is the ACF of an envelope with underlying Gaussian process with ACF

$$R_X[m] = J_1^m.$$

We call a Rayleigh process with the ACF in (12) a *first-order fading* model, following [17]. Note that we can arbitrarily set one parameter, $R_R[1]$, in the first-order model. Two different first-order models obtained by different choices of values of $R_R[1]$ are examined in the next section.

IV. Model Applications

We explore the validity of modeling the mobile radio channel with first-order fading by examining two wireless applications and comparing the results obtained from first-order fading models to the results obtained from the ISORA fading model. First-order fading with 3-dB cutoff frequency equal to the Doppler frequency is denoted the "3-dB exponential model." First-order fading with the autocorrelation points $R_X[0] = 1$ and $R_X[1] = J_1$ set equal to the ACF of the ISORA fading model is denoted the "J_1 exponential model."

The two applications considered are error correction code block-error rates and fade duration distributions. The performance of an error correction code represents a discrete-time sampled application that requires analysis over a small to moderate number of consecutive samples. The analysis of fade duration distributions represents a continuous-time application that requires analysis over a long period of time. We use simulation to obtain results for testing the results obtained from the Markov models.

A. Short Duration Application

Error correction coding is commonly used to reduce the raw channel-error rate on a fading channel from an unacceptably high value to a value acceptable to an end user. We consider two classes of codes in our examples: repetition codes and perfect error correcting codes. These classes are chosen in order to facilitate the study, but give nonetheless meaningful results.

Repetition codes are useful on fading channels and are employed in, for example, the North American Advanced Mobile Phone Service (AMPS) Control protocol [30]. Multiple identical bits are sent in series over the mobile radio channel and the receiver decision is based on majority logic. We consider 7-bit and 15-bit repetition codes. The following analysis assumes binary phase-shift keying modulation with unit variance Gaussian noise, so that the probability of bit error is

$$\Pr\{\text{Bit } n \text{ in error}\} = Q\left(\sqrt{2R_n^2}\right)$$

where $Q(\cdot)$ is the Q-function [5, eq. (2-1-97)]. A block error occurs for repetition codes when a majority of the bits in a block are in error. The variance of the Rayleigh process is set such that the probability of a block error is in the range of 0.1–0.001.

Fig. 4 shows the probability of 7-bit block errors, for the three unit-variance Rayleigh processes as a function of the Doppler spread normalized to the sampling period (bit duration). The three processes' 7-bit block-error rates are not equivalent for every Doppler frequency. For very slowly fading and fast fading channels, the three processes' block-error rates converge. The block-error rate of the J_1 model is closer to the error rate of the ISORA model than the error rate of the 3-dB model.

The ACFs over seven sample separations ($m = 0$ to 6) of the three fading models are plotted in Fig. 5 for $f_DT = 0.005$, $f_DT = 0.07$, and $f_DT = 0.4$. For the very slowly fading

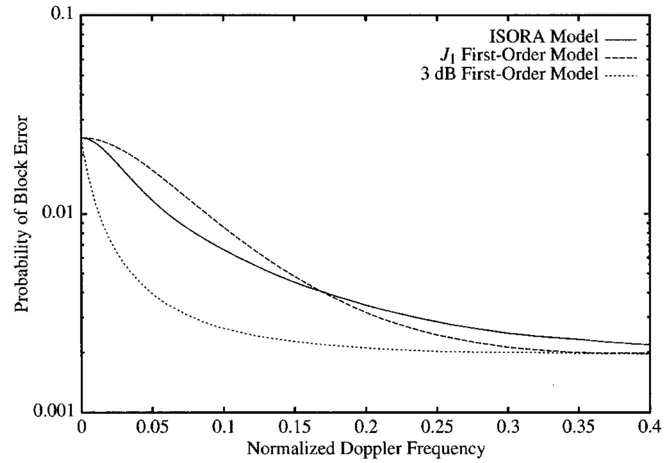

Fig. 4. Probability of a 7-bit block error with a repetition code.

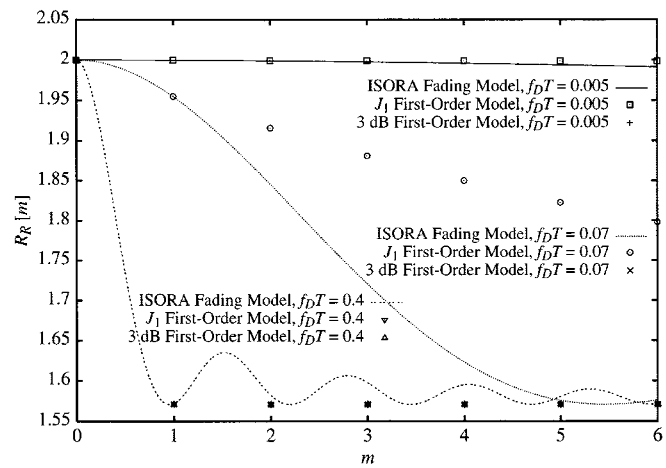

Fig. 5. Comparison of ACFs of the ISORA fading model and the J_1 exponential model at $f_DT = 0.005$, $f_DT = 0.07$, and $f_DT = 0.4$.

channel when $f_DT = 0.005$, the J_1 exponential model's ACF and the ISORA fading model's ACF are very close over seven sample separations. The number of sample separations are small relative to the first zero-crossing of the Bessel function. This is reflected in Fig. 4 as the J_1 and ISORA models' block-error rates converge for slowly fading channels. The block-error rates converge to that of a 7-bit repetition code system with completely correlated fading

$$\begin{aligned}\Pr\{\text{Block Error}\} &= \int_0^\infty \Pr\{\text{Block Error given all bits have} \\ &\qquad \cdot \text{ amplitude } r\} f_R(r)\, dr \\ &= \int_0^\infty \sum_{n=m_b}^{N_b} \binom{N_b}{n} Q\left(\sqrt{2r^2}\right)^n \\ &\qquad \cdot \left(1 - Q\left(\sqrt{2r^2}\right)\right)^{N_b - n} \frac{r}{b_0} \exp\left(-\frac{r^2}{2b_0}\right) dr\end{aligned}$$

where for 7-bit blocks, $N_b = 7$ and $m_b = 4$.

For fast fading channels, the ACF for both models approaches that of an uncorrelated model over any fixed sample separation as the fading rate increases, which is again reflected in the ACF

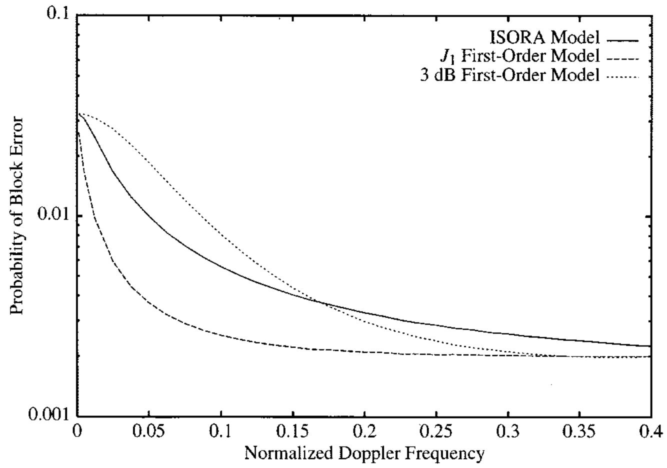

Fig. 6. Probability of a 15-bit block error with a repetition code.

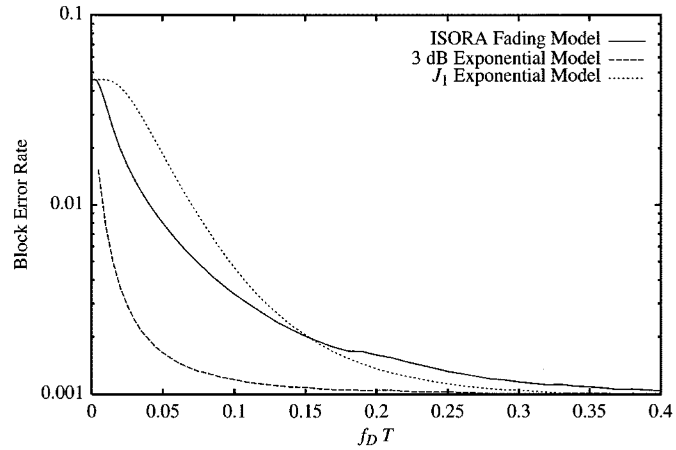

Fig. 7. Probability of a 23-bit block error with a perfect code.

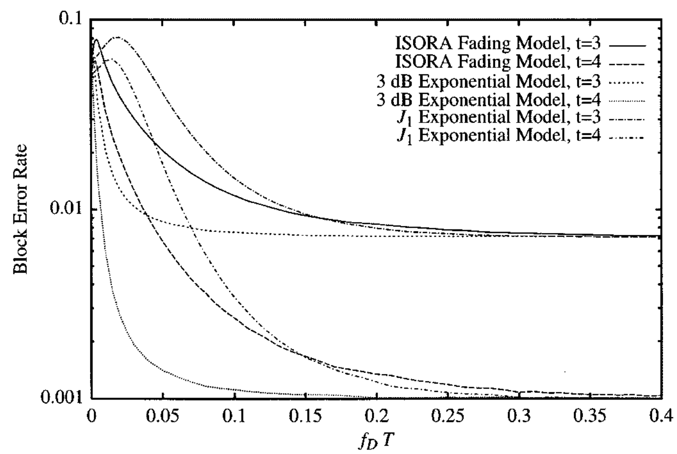

Fig. 8. Probability of a 63-bit block error with a perfect code.

in Figs. 4 and 5 when $f_D T = 0.4$. The block-error rates converge to that of a 7-bit repetition code system with independent fading

$$\Pr\{\text{Block Error}\} = \sum_{n=m_b}^{N_b} \binom{N_b}{n} P_e^n (1-P_e)^{N_b-n}$$

where P_e is the probability of bit error given the bit has amplitude r

$$P_e = \int_0^\infty Q\left(\sqrt{2r^2}\right)\frac{r}{b_0}\exp\left(-\frac{r^2}{2b_0}\right)dr = \frac{\sqrt{2b_0+1}-\sqrt{2b_0}}{2\sqrt{2b_0+1}}.$$

Although a first-order fading model sufficiently describes a fast fading channel, an uncorrelated model is even simpler to analyze. Thus, we conclude that a first-order fading model is not as useful as an uncorrelated model for fast fading.

For medium rate fading at $f_D T = 0.07$, the models exhibit greater ACF differences, which mirrors the difference in block-error rates at that Doppler frequency. A comparison of the ACFs of the exponential and ISORA fading model over the number of consecutive bits required for the application's analysis helps us predict whether the results from the two models will be close.

As the number of sample separations increases, it becomes increasingly difficult to approximate the Bessel function by an exponential function. Fig. 6 shows the probability of a 15-bit block error with the three Rayleigh processes with the variance of the Rayleigh process set such that, for fast fading, the probability of block error is equal to that in Fig. 4. There is a greater difference between the block-error rates of the first-order processes and the ISORA channel due to the increased number of consecutive samples used in the decision. Again, the J_1 model's 15-bit block-error rate is closer than the 3-dB model's rate to the ISORA model's rate. Accurate modeling of the error dependencies for moderate rate fading will thus require higher-order Markov chains or hidden Markov models.

Some wireless systems use longer codes, for which the decoding is more computationally intensive. A convenient device to faciliate discussion is to simulate perfect error correcting codes, which have much simpler decoding algorithms. Perfect codes are those which attain the Hamming bound [32]. We consider four perfect codes. The perfect (23, 12) Golay code has low latency, and has been used in mobile communications and deep space applications [33, vol. II, ch. 25]. To look at codes of larger size, we contrive hypothetical triple- and quadruple-error perfect codes of length 63, 127, and 255. Note that the performance of a practical triple-error correcting code of one of these lengths can be estimated to be between the performance bounds given by the corresponding hypothetical triple-error and quadruple-error correcting perfect codes, as practical triple-error correcting codes correct some but not all combinations of quadruple errors.

Fig. 7 shows the Golay code block-error rate as a function of the Doppler spread normalized to the sampling period as predicted by the three models. The differences between the block-error rates of the ISORA model and the Markov models are greater than for the length 7 and length 15 codes. For example, at $f_D T = 0.2$, the error rate of the J_1 model is 2.1 times the error rate of the ISORA model, and 5.5 times the error rate of the 3-dB model.

The discrepancies of the three models generally (though not strictly) increase for the longer codes. Fig. 8 shows the probability of block error for 63-bit triple-error and quadruple-error correcting perfect codes. Note that the mode of the J_1 model no longer coincides with the mode of the ISORA model. Fig. 9 shows the block-error rate of 127-bit triple-error and quadruple-error correcting perfect codes, and Fig. 10 shows the block-error rate of similar 255-bit codes. The discrepancies between the

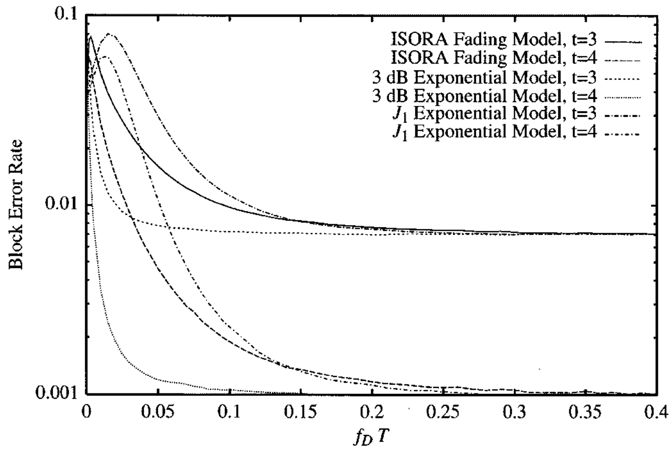

Fig. 9. Probability of a 127-bit block error with a perfect code.

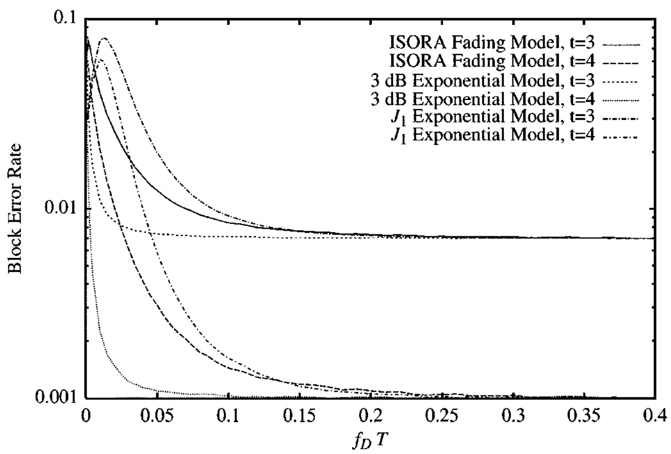

Fig. 10. Probability of a 255-bit block error with a perfect code.

TABLE I
RATIO OF PREDICTED ERROR RATES FOR PERFECT CODES AT $f_DT = 0.02$

Code Length	Errors Correctable	Ratio between ISORA and J_1 model	Ratio between ISORA and 3 dB model
7	3	1.1	2.7
15	7	1.5	2.8
23	3	2.1	5.5
63	3	2.0	3.1
63	4	3.0	7.0
127	3	2.4	3.2
127	4	3.6	7.6
255	3	2.6	3.0
255	4	4.0	7.0

block-error rates predicted by the Markov models and those predicted by the ISORA model, expressed as a ratio greater than 1, at $f_DT = 0.02$ are given in Table I. This is the value of f_DT used in Fig. 3. We observe in Fig. 3 that for adequate quantization of the fading amplitude ($N \geq 200$), the autocorrelation of the AFSMC model is "reasonably close" to that of the ISORA model for $m = 0$ to about $m = 10$. For $m \geq 15$ there is poor agreement in Fig. 3, and we note that there is also poor agreement between the models in Table I for codes longer than 15 bits ($m \geq 15$).

One further trend observed as the code length is increased is that the code performances as predicted by the three models diverge at smaller values of f_DT. Since longer codes capture more of the fading (are subject to more signal fluctuations across the length of the code), it is to be expected that they will show greater discrepancies than shorter codes, until the code length is long enough that close to full averaging of the fading takes place and the performances converge again.

B. Long Duration Application

The fade duration distribution problem shows how correlation over a long period of time can affect system analysis. The fade duration is the period of time a Rayleigh process's received signal power spends below a threshold R, where R is the fading margin. The probability distribution of the fade duration is of interest for developers of coding and modulation techniques [34], [35]. Currently, there are no general theoretical expressions for the fade duration distribution. Expressions have only been given that approximate the distribution for very shallow and very deep fades [36]. An analytical expression for the fade duration distribution would accelerate design time, give greater insight into the relationships between channel and transmission parameters, and simplify further analysis. A Markov model may yield an analytical expression for the fade duration distribution based on Mason's rule [37]. Prior to using an AFSMC model and Mason's rule to determine a fade duration distribution, we test the validity of such a solution through simulation.

Determining fade duration distributions by computer simulation requires discrete-time approximations of a continuous-time phenomena. The bandwidth of the simulation must be great enough that the average length of each fade in discrete-time units approaches the theoretical average fade duration [8, eq. (1.3-43)] $E[\tau]$, given by

$$E[\tau] = b_0\sqrt{\frac{2\pi}{b_2}}\,\frac{\exp\left(\dfrac{R^2}{2b_0}\right) - 1}{R} \tag{13}$$

where b_0 is the variance of the underlying Gaussian process, R is the fade threshold, and b_2 is the second moment of the power spectral density

$$b_2 = -\frac{\partial^2}{\partial\tau^2} R_X(\tau).$$

For the ISORA ACF

$$b_2 = \frac{b_0}{2}(2\pi f_D)^2$$

and a normalized Doppler frequency of $f_DT = 0.001$ allows sufficient bandwidth. However, for the exponential ACF

$$\begin{aligned} b_2 &= (2\pi)^2 \int_{-\infty}^{\infty} \mathcal{F}\{R_X(\tau)\} f^2\, df \\ &= (2\pi)^2 \int_{-\infty}^{\infty} \frac{4\pi f_D f^2}{(2\pi f_D)^2 + (2\pi f)^2}\, df = \infty. \end{aligned}$$

Thus, if the first-order fading model is used to calculate the average fade duration, one obtains the result $E[\tau] = 0$ [from (13)], which is incorrect.

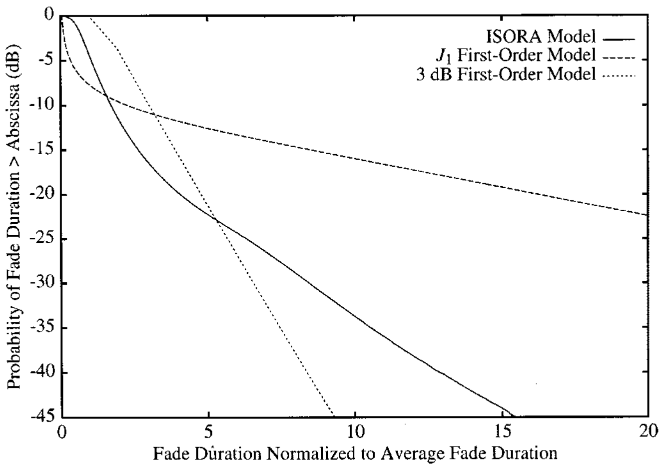

Fig. 11. Fade duration distribution for a −10-dB fading margin.

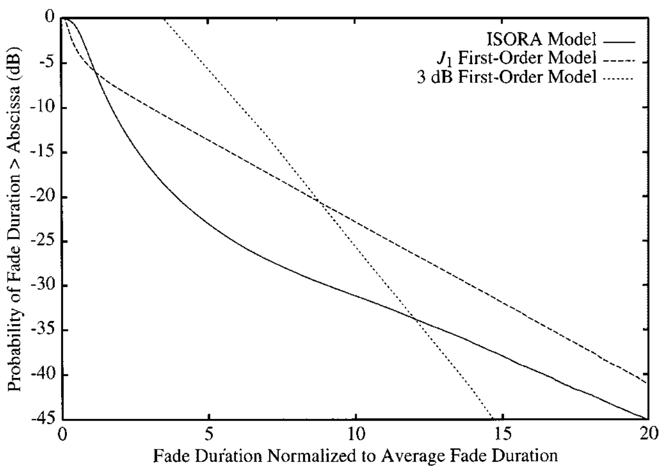

Fig. 12. Fade duration distribution for a −15-dB fading margin.

Fade duration distributions for the ISORA, J_1, and 3-dB models are presented for fades 10 dB below the mean signal level in Fig. 11 and for fades of 15 dB below the mean signal level in Fig. 12. The ordinate of both figures is the fade duration, normalized by the observed mean fade duration of each model [38]. For the 3-dB model, the bandwidth of the system is so high that the majority of the fades are one discrete-time unit long, giving it a coarse distribution curve. Clearly, the first-order models are unsuitable to model fade duration distributions, as all three curves are distinct.

The fade duration distribution application illustrates the effect of using a first-order fading model instead of using the ISORA fading model for wireless applications involving analysis over a large number of consecutive samples. Interestingly, whereas the J_1 model is closer to the ISORA model for the repetition code application and the 15-dB fade duration distribution, the 3-dB model is closer to the ISORA model for the 10-dB fade duration distribution. In contrast to Wang and Chang's results, the three models do not give equivalent results for very slowly fading channels, when $f_DT = 0.001$. We conclude that present first-order AFSMC models are not suited for this application.

The ACFs for the fade duration distribution application are shown in Fig. 13. The ACF of the J_1 and 3-dB first-order fading

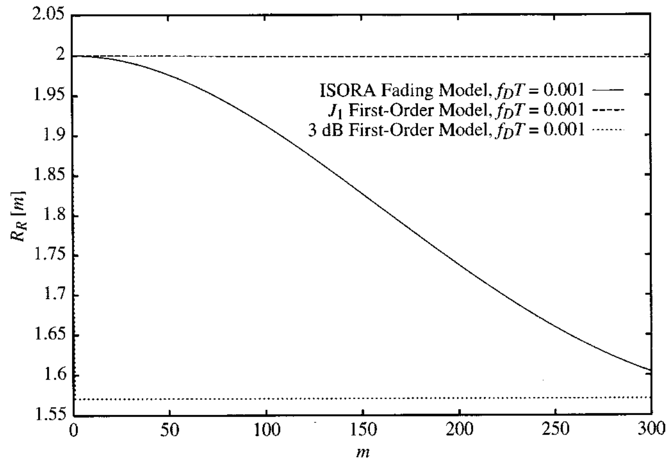

Fig. 13. Comparison of autocorrelation functions for the ISORA fading model and the J_1 exponential model at $f_DT = 0.001$.

model and of the ISORA fading model for $f_DT = 0.001$ are plotted for a large number of consecutive sample separations. The ACFs for the ISORA fading model and the first-order fading models do not agree in Fig. 13. Again, a comparison of the ACFs of the first-order and ISORA fading models over the number of consecutive bits required for the application's analysis is more significant an indicator of the usefulness of the first-order fading model than the information theoretic metric. A word of caution is appropriate here. Our examples indicate that ACF comparisons are useful as indicators of the validity of the first-order fading model. In some problems where the behavior of higher-order moments significantly influences system behavior, comparisons of the ACFs alone may be inadequate. In such cases, more complicated methods may be required.

V. Conclusion

The validity of first-order AFSMCs for the Rayleigh, flat-fading wireless channel has been examined. For applications requiring fewer consecutive samples, a first-order AFSMC can be useful only in modeling very slowly fading channels. For fast fading, an uncorrelated model may be simpler and more suitable than a first-order AFSMC. For applications requiring a large number of consecutive samples, a first-order AFSMC is typically unsuitable.

To judge when an AFSMC model is valid, a test based on comparing ACFs over the number of consecutive samples required for an application appears more effective than the information theoretic metric of Wang and Chang.

References

[1] R. H. Clarke, "A statistical theory of mobile-radio reception," *Bell Syst. Tech. J.*, vol. 47, no. 6, pp. 957–1000, 1968.

[2] M. J. Gans, "A power-spectral theory of propagation in the mobile radio environment," *IEEE Trans. Veh. Technol.*, vol. VT-21, pp. 27–38, Feb. 1972.

[3] M. Abramowitz and I. A. Stegun, *Handbook of Mathematical Functions with Formulas, Graphs, and Mathematical Tables*, 9th ed. New York: Dover, 1972.

[4] W. B. Davenport Jr. and W. L. Root, *An Introduction to the Theory of Random Signals and Noise*. New York: IEEE Press, 1958.

[5] J. G. Proakis, *Digital Communications*, 3rd ed. New York: McGraw-Hill, 1995.

[6] T. Aulin, "A modified model for the fading signal at a mobile radio channel," *IEEE Trans. Veh. Technol.*, vol. VT-28, pp. 182–203, Aug. 1979.

[7] J. D. Parsons and A. M. D. Turkmani, "Characterization of mobile radio signals: Model description," *Proc. Inst. Elect. Eng. I*, vol. 138, no. 6, pp. 549–555, 1991.

[8] W. C. Jakes, *Microwave Mobile Communications*. New York: IEEE Press, 1974.

[9] F. Swarts and H. C. Ferreira, "Markov characterization of channels with soft decision outputs," *IEEE Trans. Commun.*, vol. 41, pp. 678–682, May 1993.

[10] G. L. Stüber, *Principles of Mobile Communication*. Boston, MA: Kluwer, 1996.

[11] P. A. Bello and B. D. Nelin, "The influence of fading spectrum on the binary error probabilities of incoherent and differentially coherent matched filter receivers," *IEEE Trans. Commun.*, vol. COM-10, pp. 160–168, June 1962.

[12] H. S. Wang and N. Moayeri, "Modeling, capacity, and joint source/channel coding for Rayleigh fading channels," in *Proc. IEEE Vehicular Technology Conf. (VTC)*, Secaucus, NJ, May 1993, pp. 473–479.

[13] ——, "Finite-state Markov channel—A useful model for radio communication channels," *IEEE Trans. Veh. Technol.*, vol. 44, pp. 163–171, Feb. 1995.

[14] H. S. Wang and P.-C. Chang, "On verifying the first-order Markovian assumption for a Rayleigh fading channel model," *IEEE Trans. Veh. Technol.*, vol. 45, pp. 353–357, May 1996.

[15] M. Zorzi, R. R. Rao, and L. B. Milstein, "ARQ error control for fading mobile radio channels," *IEEE Trans. Veh. Technol.*, vol. 46, pp. 445–455, May 1997.

[16] H. Steffan, "Adaptive generative radio channel models," in *Proc. IEEE Int. Symp. Personal, Indoor and Mobile Radio Communications (PIMRC)*, The Hague, The Netherlands, Sept. 1994, pp. 268–273.

[17] H. Bischl and E. Lutz, "Packet error rate in the noninterleaved Rayleigh channel," *IEEE Trans. Commun.*, vol. 43, pp. 1375–1382, Feb./Mar./Apr. 1995.

[18] A. J. Goldsmith and P. P. Varaiya, "Capacity, mutual information, and coding for finite-state Markov channels," *IEEE Trans. Inform. Theory*, vol. 42, pp. 868–886, May 1996.

[19] F. Babich and G. Lombardi, "A measurement based Markov model for the indoor propagation channel," in *Proc. IEEE Int. Vehicular Technology Conf. (VTC)*, Phoenix, AZ, May 1997.

[20] ——, "On verifying a first-order Markovian model for the multi-threshold success/failure process for Rayleigh channel," in *Proc. IEEE Int. Symp. Personal, Indoor and Mobile Radio Communications (PIMRC)*, Helsinki, Finland, Sept. 1997.

[21] R. Dube, C. D. Rais, and S. K. Tripathi, "Improving NFS performance over wireless links," *IEEE Trans. Comput.*, vol. 46, pp. 290–298, Mar. 1997.

[22] M. Zorzi and R. R. Rao, "Error control and energy consumption in communications for nomadic computing," *IEEE Trans. Comput.*, vol. 46, pp. 279–289, Mar. 1997.

[23] L. Li and A. J. Goldsmith, "A decision-feedback maximum-likelihood decoder for fading channels," in *Proc. IEEE Global Communication Conf. (GLOBECOM)*, Phoenix, AZ, Nov. 1997, pp. 332–336.

[24] F. Babich, O. E. Kelly, and G. Lombardi, "A variable-order discrete model for the fading channel," in *Proc. IEEE 9th Thyrrenian Int. Workshop on Digital Communications*, Levici, Italy, Sept. 1997.

[25] W. Turin and R. van Nobelen, "Hidden Markov modeling of fading channels," in *Proc. IEEE Vehicular Technology Conf. (VTC)*, Ottawa, ON, Canada, May 1998, pp. 1234–1238.

[26] C. C. Tan, "On Markov modeling of fading channels," M.S. thesis, Queen's Univ., Kingston, Canada, 1997.

[27] J. G. Kemeny and J. L. Snell, *Finite Markov Chains*. Princeton, NJ: Van Nostrand, 1960.

[28] C. C. Tan and N. C. Beaulieu, "Infinite series representations of the bivariate Rayleigh and Nakagami-m distributions," *IEEE Trans. Commun.*, vol. 45, pp. 1159–1161, Oct. 1997.

[29] T. M. Cover and J. A. Thomas, *Elements of Information Theory*. New York: Wiley, 1991.

[30] Z. C. Fluhr and P. T. Porter, "Advanced mobile phone service (AMPS): Control architecture," *Bell Syst. Tech. J.*, vol. 58, no. 1, pp. 43–70, 1979.

[31] T. Delve and M. Mulligan, "Communication-systems error simulation resolves trade-offs," *EDN Access Mag.*, June 18, 1998.

[32] S. Lin and D. Costello, *Error Control Coding*. New York: Prentice-Hall, 1982.

[33] V. S. Pless and W. Huffman, *Handbook of Coding Theory*. New York: Elsevier, 1999.

[34] K. Otani, K. Daikoku, and H. Omori, "Burst error performance encountered in digital land mobile radio channel," *IEEE Trans. Veh. Technol.*, vol. VT-30, pp. 156–160, Nov. 1981.

[35] M. R. Karim, "Transmission of digital data over a Rayleigh fading channel," *IEEE Trans. Veh. Technol.*, vol. VT-31, pp. 1–6, Feb. 1982.

[36] S. O. Rice, "Distribution of the duration of fades in radio transmission: Gaussian noise model)," *Bell Syst. Tech. J.*, vol. 37, no. 3, pp. 581–635, 1958.

[37] W. W. Choy, "New results on decision feedback equalization recovery times and error rates," M.S. thesis, Queen's Univ., Kingston, ON, Canada, 1994.

[38] A. Vigants, "Number and duration of fades at 6 and 4 GHz," *Bell Syst. Tech. J.*, vol. 50, no. 3, pp. 815–841, 1971.

Christopher C. Tan (S'91–M'98) received the B.Sc. degree in electrical engineering and the B.Sc. degree in computer science from the University of Saskatchewan, Saskatoon, SK, Canada, in 1995. He served as the 1995 IEEE Student Branch Chair and received the 1995 Governor-General's Silver Medal for being the top undergraduate at the University of Saskatchewan. He received the M.Sc. degree in electrical engineering from Queen's University, Kingston, ON, Canada, in 1997. He received the 1997 award for the most outstanding postgraduate thesis in engineering and applied science at Queen's University.

In 1998, he held a research position with the Queen's Wireless Communications, Information Theory, and Communication Theory Laboratory, Queen's University, Kingston, ON, Canada, and held an adjunct postgraduate teaching position with the Department of Electrical and Computer Engineering at Queen's University. In 1999, he joined Calimetrics, Alameda, CA, as an Engineer, and currently works on digital communications system modeling, development, and implementation. Since 2000, he has held the position of Senior Engineer at Calimetrics.

Norman C. Beaulieu (S'82–M'86–SM'89–F'99) received the B.A.Sc. (honors), M.A.Sc., and Ph.D. degrees in electrical engineering in 1980, 1983, and 1986, respectively, from the University of British Columbia, Vancouver, BC, Canada. In 1980, he was awarded the University of British Columbia Special University Prize in Applied Science.

He held an appointment as Queen's National Scholar Assistant Professor in the Department of Electrical Engineering at Queen's University, Kingston, ON, Canada, from September 1986 to June 1988. From July 1988 to June 1993, he held the position of Associate Professor, and from July 1993 to August 2000, the position of Professor, both at Queen's University. In September 2000, he became the iCORE Research Chair in Broadband Wireless Communications at the University of Alberta, Edmonton, AB, Canada. His current research interests include digital communications over fading channels, interference effects in digital modulations, channel modeling and simulation, decision-feedback equalization, and digital synchronization in sampled receivers.

Dr. Beaulieu is a member of the IEEE Communication Theory Committee. He served as representative of the Communication Theory Committee to the Technical Program Committee of the 1991 International Conference on Communications and as co-representative of the Communication Theory Committee to the Technical Program Committee of the 1993 International Conference on Communications and the 1996 International Conference on Communications. He was General Chair of the Sixth Communication Theory Mini-Conference in association with GLOBECOM'97, and Co-Chair of the Canadian Workshop on Information Theory 1999. Since January 1992, he has served as Editor for Wireless Communication Theory of the IEEE TRANSACTIONS ON COMMUNICATIONS. Since November 1996, he has served as Associate Editor for Wireless Communication Theory of the IEEE COMMUNICATIONS LETTERS. Effective January 2000, Dr. Beaulieu was appointed Editor-in-Chief of the IEEE TRANSACTIONS ON COMMUNICATIONS. He was a recipient of the Natural Science and Engineering Research Council (NSERC) E.W.R. Steacie Memorial Fellowship in 1999.